ARCHIVES OF ELECTRICAL ENGINEERING VOL. 71(2), pp. 471–488 (2022)

DOI 10.24425/aee.2022.140723

Effects of harmonics and voltage unbalance on the behavior of a five-phase permanent magnet synchronous machine

AHMED AMINE KEBIR ✉, MOULOUD AYAD, SAOUDI KAMEL

LPM3E Laboratory, Faculty of Sciences and Applied Sciences, University of Bouira Algeria

e-mails: {✉a.kebir/m.ayad/k.saoudi}@univ-bouira.dz

(Received: 11.09.2021, revised: 24.01.2022)

Abstract: The development in industrial systems leads to the augmentation in the consumption of the power. Therefore, this development makes use of multiphase machines. The use of multiphase machines caused several problems and defects. Electrical energy is mainly distributed in a three-phase system to provide the electrical power necessary for the electrical engineering equipment and materials. The sinusoidal aspect of the required original voltage primarily preserves its essential qualities for transmitting useful power to terminal equipment. When the voltage waveform is no longer sinusoidal, perturbations are encountered, which generate malfunctions and overheating of the receivers and the equipment connected to the same electrical supply network. The main disturbing phenomena are harmonics, voltage fluctuations, voltage unbalances, electromagnetic fields, and electrostatic discharges. This present work aims to study the effects of harmonic pollution and voltage unbalance on the five-phase permanent magnet synchronous machine using spectrum current analysis and wavelet transform.

Key words: fault detection, five-phase permanent magnet synchronous machine (FPPMSM), harmonics, spectrum analysis, voltage unbalance

1. Introduction

Recently, the increasing use of power electronic devices in electrical systems has led to enormous harmonic disturbances or distortions in electrical networks. This phenomenon affects all industrial, tertiary, and domestic sectors using non-linear loads [1, 2]. These non-linear loads, on one hand, absorb non-sinusoidal currents, which circulate in the power lines and distort the grid voltage through the short-circuit impedance of the line. On the other hand, they consume reactive power, which has the consequence of degrading the power factor. The harmonics generated are permanent disturbances affecting the waveform of the voltage and current of the network. These disturbances are superimposed on the fundamental wave. Therefore, the effect of the harmonics is the modification of the voltage or current wave. The consequence is the degradation of the power factor by the generation of alternating currents and voltages with frequencies different from the fundamental. Current and voltage deformations naturally have harmful consequences on electrical equipment, ranging from an intense heating or sudden stoppage of rotating machines to the destruction of this equipment [3–6]. Several previous works have deeply studied the five-phase permanent magnet synchronous machine and have shown their advantages over the regular three-phase permanent magnet synchronous machine with different approaches [7–9].

In the literature, we find fewer studies on the effects of harmonics and voltage unbalance on the behaviour of the five-phase synchronous machine compared to the three-phase machine, which was studied using several methods and different approaches [10–13].

The authors in paper [10] present a study about the effects of voltage unbalance and harmonics on a three-phase induction motor. The effects of the three-phase voltage un-balance and harmonic under the condition of under voltage and overvoltage are investigated. In [11], the authors present the effects of voltage unbalance and harmonic distortion on the torque and efficiency of a three-phase induction motor. The behaviour of the torque and efficiency of a three-phase induction motor with unbalanced voltages and harmonic distortions is investigated. Quispe and Lopez present in [12] the effects of unbalanced voltages on the energy performance of three-phase induction motors. They have presented positive sequence voltage's influence on the line currents, losses, efficiency, and power factor under different voltage unstable conditions. Paper [13] presents an overview of multiphase energy conversion and introduces the relevant technology advances, design of multiphase, multiphase converter topologies, modelling, and control of multiphase generators.

In paper [14], the authors investigate the control of three-phase induction machine drives during open-circuit faults. It is an overview of existing control methods for three-phase induction machine drives during open-circuit faults. This paper uses the spectrum current analysis and wavelet transform to study the effects of harmonic pollution and voltage unbalance on the five-phase permanent magnet synchronous machine. Initially, the two phenomena of harmonics and voltage unbalance were defined. Then, a model of the five-phase permanent magnet synchronous machine (FPPMSM) using the coupled magnetic circuit method (CMCM) was developed, then used to monitor the effects of harmonics and voltage imbalances on the efficiency of the FPPMSM using the techniques of spectral analysis and then wavelet.

2. Methodology

2.1. The different modelling methods of electric machines

2.1.1. The finite element method (FEM)

In the numerical approach the finite element method is used for the resolution of electromagnetic field equations including the real properties of materials and complex geometric configurations. The discretization or the fine mesh of the field of study makes it possible to increase the precision of the results. However, as the requirements of numerical modelling problems evolve, some limitations of the finite element method become too restrictive. A large part of these handicaps is linked to its strong dependence on the mesh and the relating to computer resources (time and significant memory space).

2.1.2. The reluctance network method (RNM)

The reluctance network method (RNM) based on magnetic equivalent schemes has an intermediate level of complexity between two methods, the CMCM and FEM. It offers the advantage of describing more precisely the quantities of the system using a graphic representation of the geometry of the machine, including local saturation phenomena (generated by the magnets on the primary teeth). However, the very complex representation of energy exchanges in the air gap remains a major obstacle to its use.

2.1.3. Coupled magnetic circuit method (CMCM)

In the modelling approach using the coupled magnetic circuit method (CMCM), the stator's windings are represented by an equivalent electrical circuit formed by inductance in series with a resistance. The self and mutual inductances between the different stator phases are essential in this modelling method because they contain the signature of the various phenomena that may appear within the machine. These inductances can be calculated using the winding functions. This type of modelling, therefore, allows space harmonics to be taken into account even if the CMCM does not consider certain phenomena (saturation, skin effect, etc.). Thus, despite its weaknesses, the CMCM approach offers better precision, calculation time, and adaptation to modelling most faults of electromagnetic origin in electrical machines [15].

2.2. Modelling of FFPMSM by the use of CMCM

The modelling of a five-phase PMSM is as shown in Fig. 1.

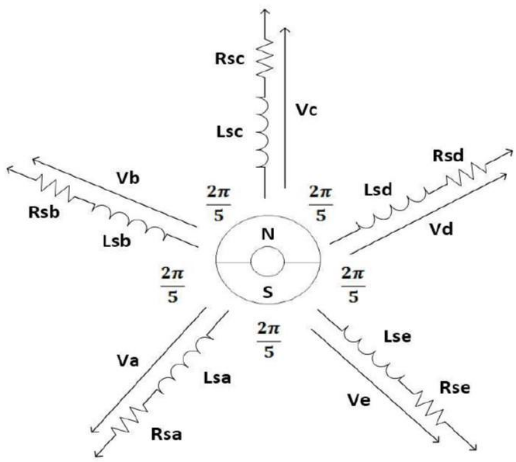

Fig. 1. Modeling of a five-phase PMSM

2.2.1. Electrical equations

The electrical model of the five-phase machine (5 phases) in the stator *abcde* frame is as follows:

$$v^s_{abcde} = R^s_{abcde} i^s_{abcde} + \frac{\mathrm{d}\varphi^s_{abcde}}{\mathrm{d}t}. \tag{1}$$

v^s_{abcde}, R^s_{abcde}, i^s_{abcde} and φ^s_{abcde} indicate the magnitudes and electromagnetic parameters of the five phases, expressed in matrix form:

$$v^s_{abcde} = \begin{bmatrix} v^s_a & v^s_b & v^s_c & v^s_d & v^s_e \end{bmatrix}^T, \tag{2}$$

$$i^s_{abcde} = \begin{bmatrix} i^s_a & i^s_b & i^s_c & i^s_d & i^s_e \end{bmatrix}^T, \tag{3}$$

$$\left[R^s_{abcde}\right] = \begin{bmatrix} R^s_a & 0 & 0 & 0 & 0 \\ 0 & R^s_b & 0 & 0 & 0 \\ 0 & 0 & R^s_c & 0 & 0 \\ 0 & 0 & 0 & R^s_d & 0 \\ 0 & 0 & 0 & 0 & R^s_e \end{bmatrix}, \tag{4}$$

$$\varphi^s_{abcde} = \begin{bmatrix} \varphi^s_a & \varphi^s_b & \varphi^s_c & \varphi^s_d & \varphi^s_e \end{bmatrix}. \tag{5}$$

2.2.2. Magnetic equations

φ^s_{abcde} can be expressed by:

$$\begin{cases} \varphi^s_a = L_s i^s_a + \varphi_{ma} \\ \varphi^s_b = L_s i^s_b + \varphi_{mb} \\ \varphi^s_c = L_s i^s_c + \varphi_{mc} \end{cases} \quad \begin{matrix} \varphi^s_d = L_s i^s_d + \varphi_{md} \\ \varphi^s_e = L_s i^s_e + \varphi_{me} \end{matrix}. \tag{6}$$

The flows are proportional to the currents, and the proper and mutual inductances only depend on the angular displacement (θ_r):

$$\begin{cases} \varphi^s_a = L_{aa} i^s_a + M_{ab} i^s_b + M_{ac} i^s_c + M_{ad} i^s_d + M_{ae} i^s_e + \varphi_{ma}(\theta_r) \\ \varphi^s_b = L_{bb} i^s_b + M_{ba} i^s_a + M_{bc} i^s_c + M_{bd} i^s_d + M_{be} i^s_e + \varphi_{mb}(\theta_r) \\ \varphi^s_c = L_{cc} i^s_c + M_{ca} i^s_a + M_{cb} i^s_b + M_{cd} i^s_d + M_{ce} i^s_e + \varphi_{mc}(\theta_r) \\ \varphi^s_d = L_{dd} i^s_d + M_{da} i^s_a + M_{db} i^s_b + M_{dc} i^s_c + M_{de} i^s_e + \varphi_{md}(\theta_r) \\ \varphi^s_e = L_{ee} i^s_e + M_{ea} i^s_a + M_{eb} i^s_b + M_{ec} i^s_c + M_{ed} i^s_d + \varphi_{me}(\theta_r) \end{cases}. \tag{7}$$

θ_r is the angular position of the rotor; L_s is the stator inductance, it is defined by the following matrix:

$$[L_s] = \begin{bmatrix} L_{aa} & M_{ab} & M_{ac} & M_{ad} & M_{ae} \\ M_{ba} & L_{bb} & M_{bc} & M_{bd} & M_{be} \\ M_{ca} & M_{cb} & L_{cc} & M_{cd} & M_{ce} \\ M_{da} & M_{db} & M_{dc} & L_{dd} & M_{de} \\ M_{ea} & M_{eb} & M_{ec} & M_{ed} & L_{ee} \end{bmatrix}, \tag{8}$$

with:

$$L_{aa} = L_{bb} = L_{cc} = L_{dd} = L_{ee} = L,$$
$$M_{ab} = M_{ac} = M_{ad} = M_{ae} = M.$$

The inductance matrix L_s becomes in the form below:

$$[L_s] = \begin{bmatrix} L & M & M & M & M \\ M & L & M & M & M \\ M & M & L & M & M \\ M & M & M & L & M \\ M & M & M & M & L \end{bmatrix}. \tag{9}$$

The matrix system which encompasses the electric equations and the magnetic equations is as follows:

$$\begin{bmatrix} v_a^s \\ v_b^s \\ v_c^s \\ v_d^s \\ v_e^s \end{bmatrix} = \begin{bmatrix} R_a^s & 0 & 0 & 0 & 0 \\ 0 & R_b^s & 0 & 0 & 0 \\ 0 & 0 & R_c^s & 0 & 0 \\ 0 & 0 & 0 & R_d^s & 0 \\ 0 & 0 & 0 & 0 & R_e^s \end{bmatrix} \begin{bmatrix} i_a^s \\ i_b^s \\ i_c^s \\ i_d^s \\ i_e^s \end{bmatrix} + \omega_r \frac{\mathrm{d}}{\mathrm{d}\theta_r} \begin{bmatrix} L & M & M & M & M \\ M & L & M & M & M \\ M & M & L & M & M \\ M & M & M & L & M \\ M & M & M & M & L \end{bmatrix} \begin{bmatrix} i_a^s \\ i_b^s \\ i_c^s \\ i_d^s \\ i_e^s \end{bmatrix}$$
$$+ \begin{bmatrix} L & M & M & M & M \\ M & L & M & M & M \\ M & M & L & M & M \\ M & M & M & L & M \\ M & M & M & M & L \end{bmatrix} \frac{\mathrm{d}}{\mathrm{d}t} \begin{bmatrix} i_a^s \\ i_b^s \\ i_c^s \\ i_d^s \\ i_e^s \end{bmatrix} + \omega_r \frac{\mathrm{d}}{\mathrm{d}\theta_r} \begin{bmatrix} \varphi_{ma}(\theta_r) \\ \varphi_{mb}(\theta_r) \\ \varphi_{mc}(\theta_r) \\ \varphi_{md}(\theta_r) \\ \varphi_{me}(\theta_r) \end{bmatrix}. \tag{10}$$

The flux produced by the permanent magnets φ_{mabcde} is related to the electrical angular position θ_r of the rotor.

The phase shift between the stator windings is $-2\pi/5$ and the distribution of flux passing through them is sinusoidal, φ_{mabcde} can then be expressed as:

$$\varphi_{mabcde}(\theta_r) = \begin{bmatrix} \varphi_{ma}(\theta_r) \\ \varphi_{mb}(\theta_r) \\ \varphi_{mc}(\theta_r) \\ \varphi_{md}(\theta_r) \\ \varphi_{me}(\theta_r) \end{bmatrix} = \varphi_m \begin{bmatrix} \sin(\theta_r) \\ \sin\left(\theta_r - \dfrac{2\pi}{5}\right) \\ \sin\left(\theta_r - \dfrac{4\pi}{5}\right) \\ \sin\left(\theta_r - \dfrac{6\pi}{5}\right) \\ \sin\left(\theta_r - \dfrac{8\pi}{5}\right) \end{bmatrix}. \tag{11}$$

The variation in flux corresponding to the electromotive forces:

$$\frac{\mathrm{d}\varphi_{mabcde}(\theta_r)}{\mathrm{d}t} = \varphi_m \omega_r \begin{bmatrix} \cos(\theta_r) \\ \cos\left(\theta_r - \frac{2\pi}{5}\right) \\ \cos\left(\theta_r - \frac{4\pi}{5}\right) \\ \cos\left(\theta_r - \frac{6\pi}{5}\right) \\ \cos\left(\theta_r - \frac{8\pi}{5}\right) \end{bmatrix}, \tag{12}$$

where ω_r is the rotation speed.

2.2.3. Mechanical equations

The mechanical model can be described by the following two equations:

$$\begin{aligned} -Cr &= J \cdot \frac{\partial \Omega r}{\partial t} + fv \cdot \omega_r - C_e, \\ 0 &= -\omega_r + \frac{\partial \theta r}{\partial t}. \end{aligned} \tag{13}$$

The expression of the electromagnetic torque C_e exerted on the rotor obtained from the stored electromagnetic energy W_{em} is given by the following relation:

$$C_e = p \left\{ \left[r^s_{abcde} \right]^T \frac{\mathrm{d}\left[\varphi_{mabcde}(\theta_r) \right]}{\mathrm{d}\theta_r} \right\}.$$

2.2.4. State model of the FPPMSM

The following equation presents the state model of the FPPMSM:

$$\begin{bmatrix} v^s_a \\ v^s_b \\ v^s_c \\ v^s_d \\ v^s_e \\ -Cr \\ 0 \end{bmatrix} = \begin{bmatrix} R^s_a & 0 & 0 & 0 & 0 & Z_1 & 0 \\ 0 & R^s_b & 0 & 0 & 0 & Z_2 & 0 \\ 0 & 0 & R^s_c & 0 & 0 & Z_3 & 0 \\ 0 & 0 & 0 & R^s_d & 0 & Z_4 & 0 \\ 0 & 0 & 0 & 0 & R^s_e & Z_5 & 0 \\ -Z_1 & -Z_2 & -Z_3 & -Z_4 & -Z_5 & f_v & 0 \\ 0 & 0 & 0 & 0 & 0 & -1 & 0 \end{bmatrix} \begin{bmatrix} i^s_a \\ i^s_b \\ i^s_c \\ i^s_d \\ i^s_e \\ \omega_r \\ \theta \end{bmatrix}$$

$$+ \begin{bmatrix} L & M & M & M & M & 0 & 0 \\ M & L & M & M & M & 0 & 0 \\ M & M & L & M & M & 0 & 0 \\ M & M & M & L & M & 0 & 0 \\ M & M & M & M & L & 0 & 0 \\ 0 & 0 & 0 & 0 & 0 & J & 0 \\ 0 & 0 & 0 & 0 & 0 & 0 & 1 \end{bmatrix} \frac{\mathrm{d}}{\mathrm{d}t} \begin{bmatrix} i^s_a \\ i^s_b \\ i^s_c \\ i^s_d \\ i^s_e \\ \omega_r \\ \theta \end{bmatrix}, \tag{14}$$

with:

$$\begin{cases} Z_1 = -\varphi_m \cdot \cos(\theta_r) & Z_4 = -\varphi_m \cdot \cos\left(\theta_r - \dfrac{6\pi}{5}\right) \\ Z_2 = -\varphi_m \cdot \cos\left(\theta_r - \dfrac{2\pi}{5}\right) & \\ Z_3 = -\varphi_m \cdot \cos\left(\theta_r - \dfrac{4\pi}{5}\right) & Z_5 = -\varphi_m \cdot \cos\left(\theta_r - \dfrac{8\pi}{5}\right) \end{cases}.$$

3. Voltage unbalance and harmonic pollution

3.1. Voltage unbalance

In a balanced system, the voltage phase should be equal or nearly equal. A voltage unbalance is the measure of the voltage differences between different phases of the system.

A system is unbalanced or asymmetrical if the voltages and currents do not have the same amplitude and/or are not out of phase. The different cases of voltage unbalance supply are: under voltage, overvoltage, phase shift [16] (Fig. 2).

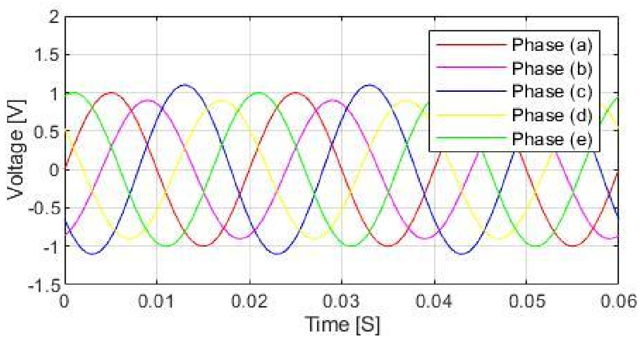

Fig. 2. Unbalanced voltages (phase (c) affected by an overvoltage of 10%, phase (b) and (c) affected by an undervoltage of 10%)

3.2. Harmonic pollution

So-called non-linear loads produce the most current harmonics. The most common of these loads are variable frequency drives (VFDs) associated with rotating machines of power electronic components. There are also types of equipment such as computers, servers, and other electronic devices, lighting with electronic loads with or without dimmers, soldering stations, and uninterruptible power supplies (UPSs), more commonly referred to as inverters [16].

The harmonic currents produced by these non-linear loads flow in the supply and the distribution networks. The impact of these harmonic currents on the impedance of these distribution networks (generally the inductive type) leads to a deformation of the sinusoidal voltage. This phenomenon is called voltage distortion.

The influence of these harmonic currents on the basic sinusoidal shape is shown in the following figure (Fig. 3). The resulting "distorted wave" signal in Fig. 4(b) is, in fact, the sum of the fundamental in Fig. 4(a) and the harmonic wave of the order "n" in Fig. 4(c).

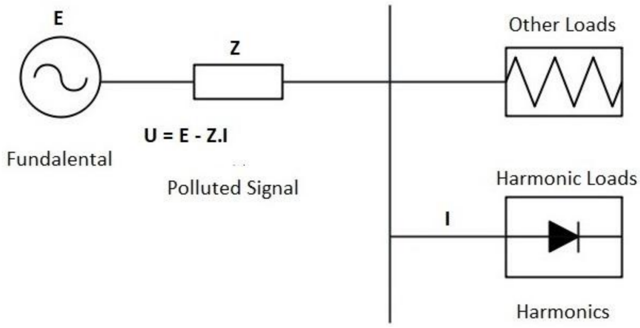

Fig. 3. Degradation of the network voltage by a non-linear load

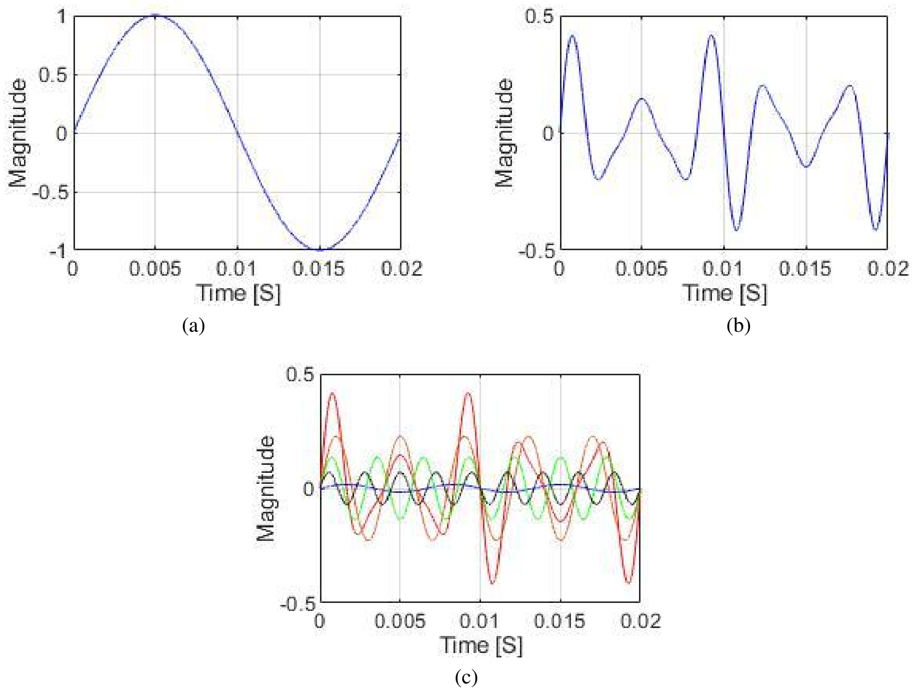

Fig. 4. The influence of harmonics on the sinisuidal shape of the signal: (a) source signal without pollution; (b) polluted signal; (c) 3^{rd}, 5^{rd}, 7^{rd}, 9^{rd} hamonic generated by non-linear loads

4. Results and discussion

From the set-up state model of the FFPMSM, the machine will be reproduced using MATLAB. Therefore, this permits us to describe the behaviour of the device by picturing diagrams of various quantities. The differential equations have resulted in the Runge-Kutta-4 method, a technique for approximating differential equation solutions. This technique depends on the principle of iteration.

4.1. Results of the model without defects in the (*abcde*) reference

Here, the results obtained by the model simulation without defects in the (*abcde*) reference are given in Fig. 5.

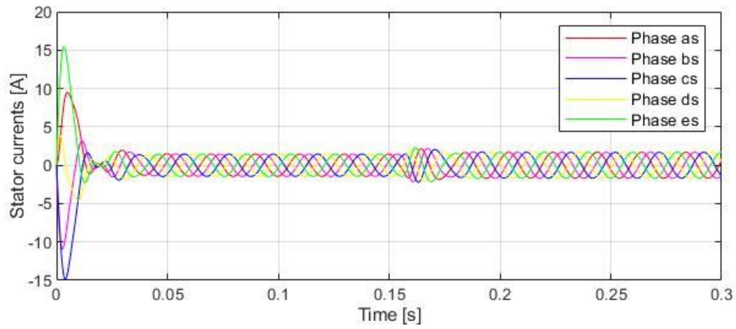

(a)

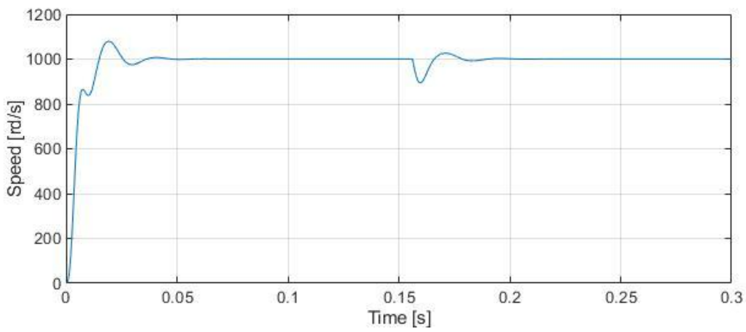

(b)

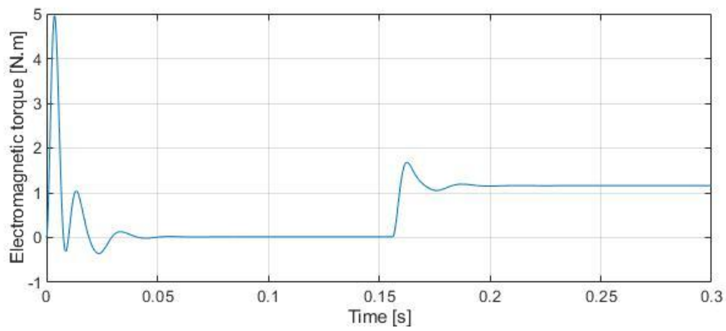

(c)

Fig. 5. The non-faulty model, (a): stator currents, (b): rotation speed, (c): electromagnetic torque

Figures 5(a), 5(b), 5(c), respectively represent the stator currents, rotation speed, electromagnetic torque of a five-phase permanent magnet synchronous machine in healthy mode as a function of time. At the instant $t = 0.16$ s a resistive load was applied to the machine.

Figure 5(a) we notice a disturbance in the stator currents when the load was applied to the machine, Fig. 5(b) we notice a disturbance in the rotation speed when the load was applied to the machine, in Fig. 5(c) we notice that the electromagnetic torque increases and becomes unstable over a short period of time.

4.2. Behaviour of the model under unbalanced voltages in the (*abcde*) reference

Figure 6 shows that the voltage imbalance generates significant increases in the current of phases b and d when it occurs at $t = 0.24$ s, with current augmentation when the resistive load is

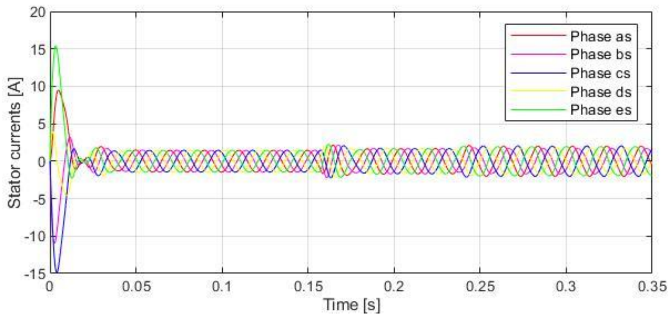

(a)

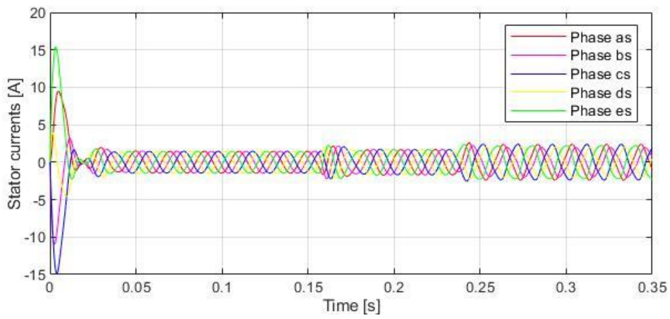

(b)

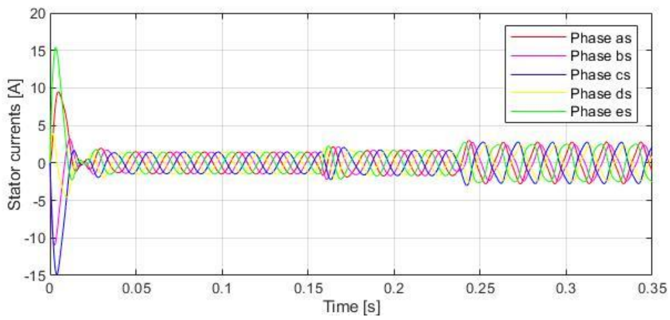

(c)

Fig. 6

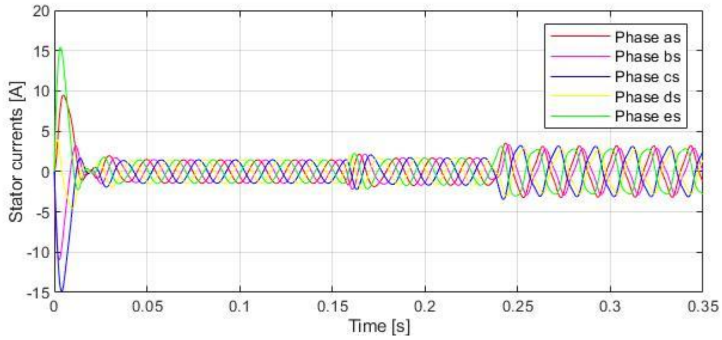

(d)

Fig. 6. The stator currents under unbalanced voltages: (a) 2.5% voltage drop in phase (a, b); (b) 5% voltage drop in phase (a, b); (c) 7.5% voltage drop in phase (a, b); (d) 10% voltage drop in phase (a, b)

applied at $t = 0.16$ s. The growth in current amplitude is greater the higher the voltage imbalance percentage is.

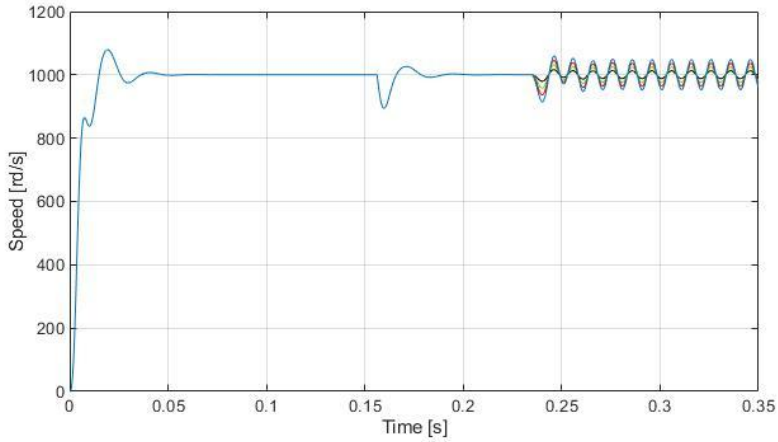

Fig. 7. The speed under unbalanced voltages (phase (b) and (d) affected with 2.5%, 5%, 7.5%, 10% drop in voltage)

Figures 8 and 10 show that the voltage unbalance generates also significant increases in rotation speed and torque of phases (b) and (d) when it occurs at $t = 0.24$ s. The growth in rotation speed and electromagnetic torque is greater the higher the voltage imbalance percentage is.

The unbalance voltage is caused primarily by loads that vary in current inrush quickly and continuously. The best-known examples are welding machines and especially arc furnaces. Variations in the unbalance voltage value can have undesirable effects on the torque and speed of rotating machinery, like the heating of rotating machines due to reverse torques (Fig. 11).

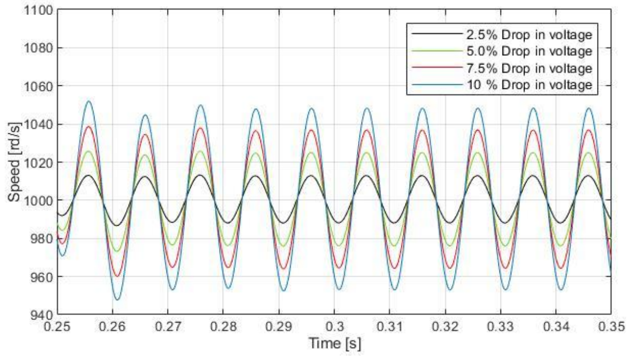

Fig. 8. Zoom of the speed under unbalanced voltages (phase (b) and (d) affected with 2.5%, 5%, 7.5%, 10% drop in voltage)

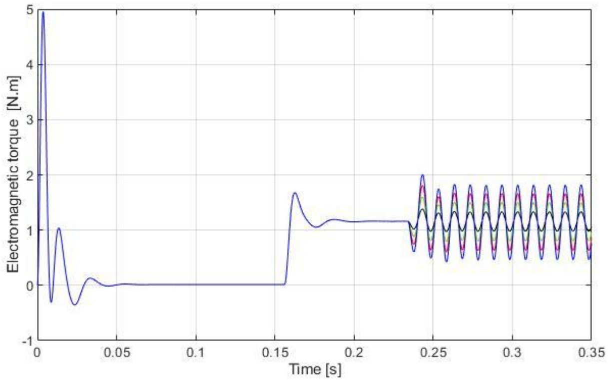

Fig. 9. The electromagnetic torque under unbalanced voltages (phase (b) and (d) affected with 2.5%, 5%, 7.5%, 10% drop in voltage)

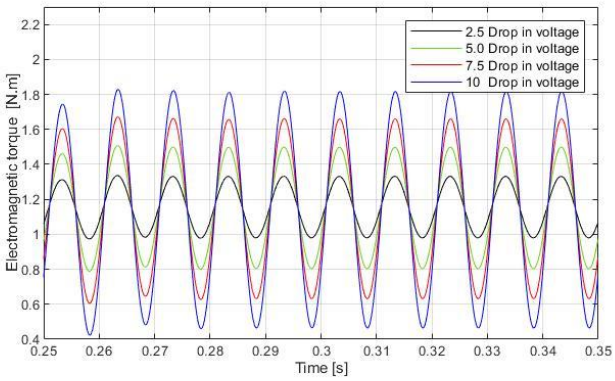

Fig. 10. Zoom of the electromagnetic torque under unbalanced voltages (phase (b) and (d) affected with 2.5%, 5%, 7.5%, 10% drop in voltage)

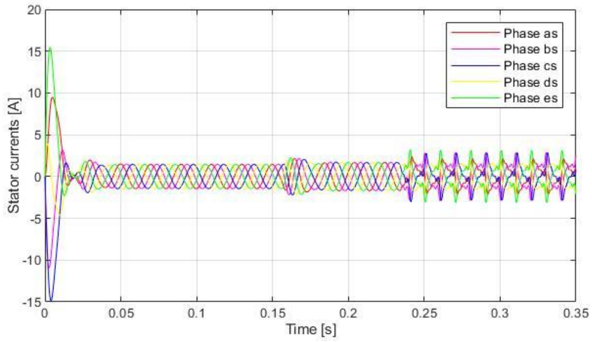

(a)

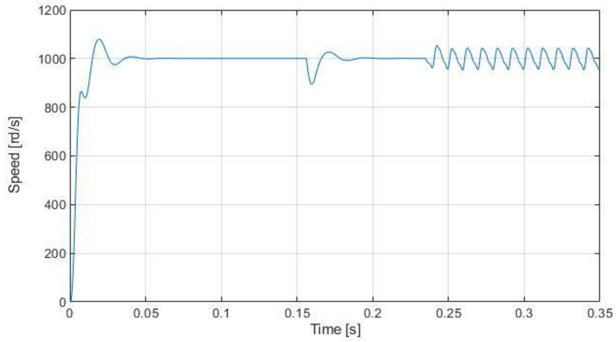

(b)

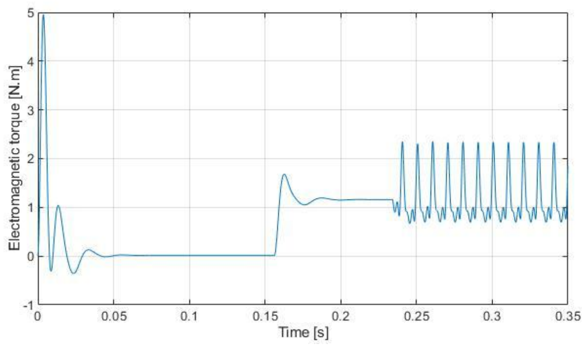

(c)

Fig. 11. Simulation results under harmonics; (a) stator currents; (b) rotation speed; (c) electromagnetic torque

4.3. Behaviour of the model under harmonic pollution in the (*abcde*) reference

It is noted that permanent oscillations and distortions appears in the current, rotation speed, and torque of the machine when applying the maximum percentage of harmonic allowed by the IEC 61000-2-2 standard, H3 = 5%, H5 = 6%, H7 = 5% and H9 = 1.5% of voltage RMS at $t = 0.23$ s.

The presence of harmonics causes vibrations and noise in electromagnetic devices. Due to rotating harmonic fields, parasitic mechanical torques give vibrations in rotating machines. The harmonics also increase iron losses (eddy current losses) and cause aging of insulators and therefore increase the current leakage or even excessive heating in the conductors.

4.4. Spectrum analysis of the stator currents

Based on fast Fourier transform (FFT), the spectral analysis of the stator current was used to extract the fault-relevant signal characteristics.

A stator current spectral analysis using the fast Fourier transform (FFT) was performed to extract the fault-relevant signal characteristics.

The spectral analysis visualized in Fig. 12(b) shows the presence of the harmonic segment of rank three identified with current twisting brought by the unbalanced voltage, as well as the presence of the segment part of ranks 3, 5, 7, and 9, in Fig. 12(c) was contained in the polluted voltage source.

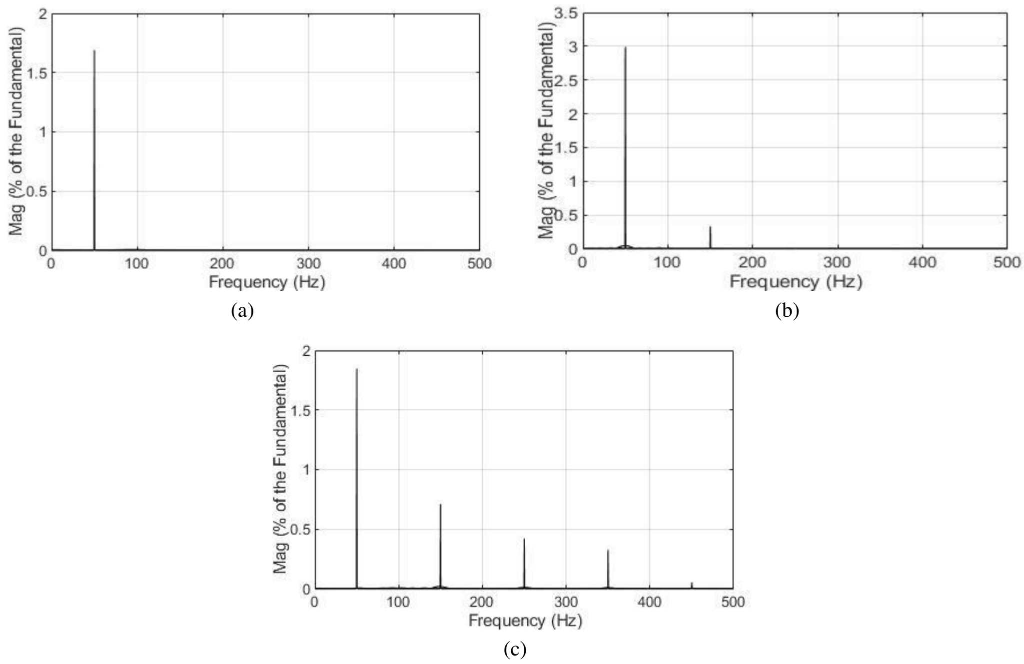

Fig. 12. Spectral analysis of stator currents: (a) without faults; (b) unbalanced voltages; (c) harmonic voltages

4.5. Wavelet analysis of the stator currents

The wavelet analysis is applied to the stator current to investigate and distinguish the voltage unbalance and the voltage harmonic pollution.

Figures 13, 14, and 15 show the wavelet analysis of the stator current in three cases, first the healthy, then with unbalanced voltages, and finally with harmonics. Detail levels of high-

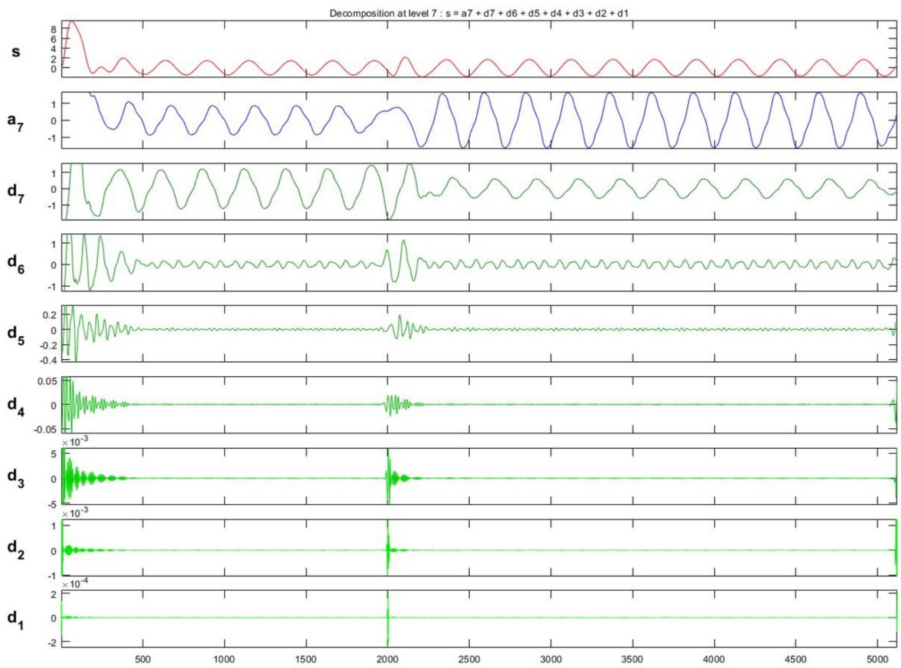

Fig. 13. Investigation of the stator current with wavelet (faults free)

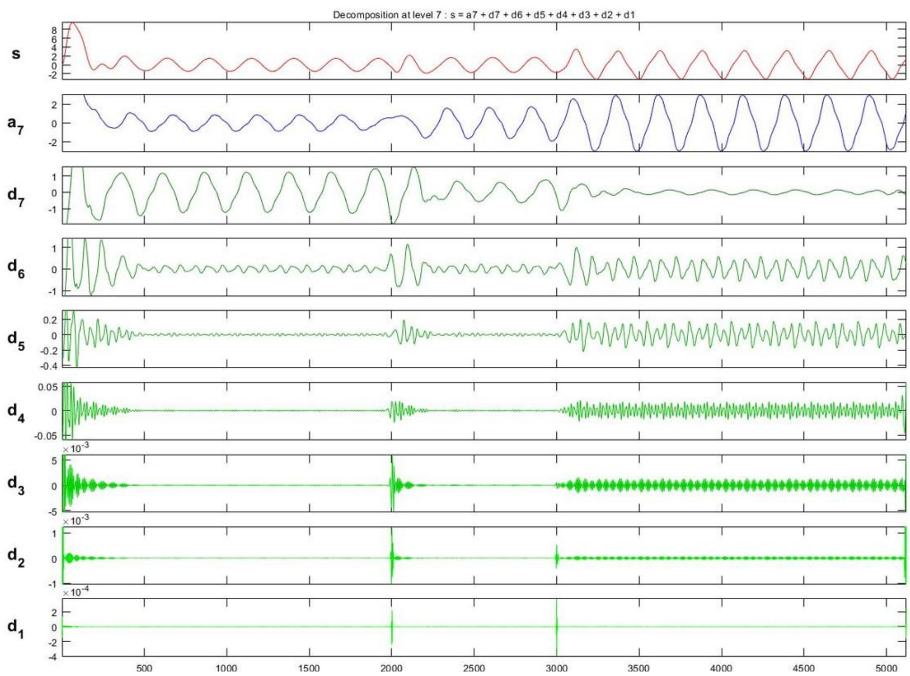

Fig. 14. Investigation of the stator current with wavelet (case of unbalanced voltages)

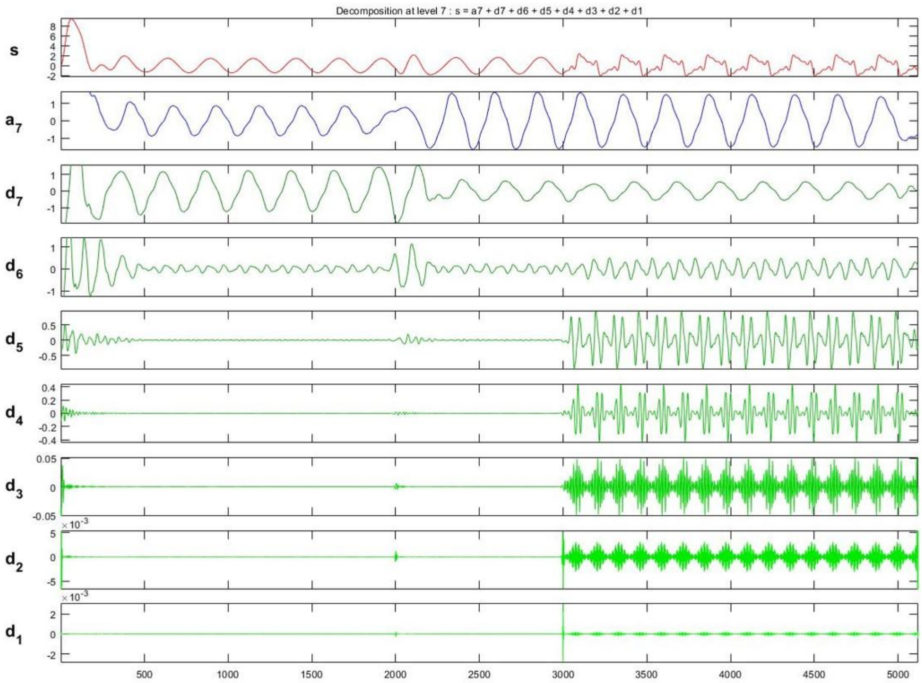

Fig. 15. Investigation of the stator current with wavelet (case of harmonic voltages)

frequency bands show no information about the original signal. But, in the low-frequency bands (d4, d5, and d6), the voltage unbalances and harmonic pollution are much more relevant because the bands cover the frequencies corresponding to the fundamental, the voltage unbalances the voltage harmonic pollution.

5. Conclusion

Electrical perturbations such as harmonics and voltage unbalance can occur in the electrical network. However, these perturbations should not be taken as a disaster. The impact of harmonic pollution and voltage unbalance on motors can be heavy. The insulation of the motor windings can deteriorate, which can lead to early and costly motor failure and unplanned downtime and energy losses in the conductors, additional Joule losses, as well as oversizing of equipment and the electrical components. The Fourier transform was for a long time one of the most used tools for signal processing. This representation, based on the physical notion of frequency, is well suited to processing stationary signals, that is to say signals which have certain properties that are time invariant. The main limitation of the Fourier transform is that it does not allow a local description (over a finite part) of a signal. To remedy these limitations, the so-called time-frequency, representations have been proposed such as the wavelet in order to analyse a signal using a transformation parameterized by two variables: time (or position) and frequency (or ladder). The goal of the work was to study the electrical perturbations and identify them, then apply them and identify their effects on the behaviour of the FPPMSM. To achieve this goal, a state model of the FPPMS was created and solved in MATLAB using the Rang-Kutta method; finally, a spectral analysis (FFT) and a wavelet analysis of stator current were carried out.

Appendix

Table 1. FPPMSM Data

Parameter name	**Symbol**	**Value**	**Unit**
Stator Inductance	L_s	0.0032	H
Stator Resistance	R_s	1.4	
Mutual	M	–0.00013	
Rated Speed	W_r	1000	rpm
Polepair	P	3	
Magnetic flux	$\emptyset$	0.3	Wb
Inertia	J	0.00065	kg·m^2
Frequency	F	50	Hz
Voltage	V	33	V

References

[1] Dao T., Phung B.T., *Effects of voltage harmonic on losses and temperature rise in distribution transformers*, IET Generation, Transmission and Distribution, vol. 12, no. 2, pp. 347–354 (2018), DOI: 10.1049/iet-gtd.2017.0498.

[2] Lee C.Y., Lin Y.J., Chen C.R., *The effect of harmonic phase angle on the operation performance of a three-phase induction motor*, IEEE Power Engineering Society Summer Meeting (Cat. No. 00CH37134), vol. 4, pp. 2499–2505 (2000), DOI: 10.1109/PESS.2000.867384.

[3] Jaeger M., Drichel P., Schröder M., Berroth J., Jacobs G., Hameyer K., *On magnetization deviations as the dominant cause for vibration harmonics in the spectrum of a PMSM drive*, Archives of Electrical Engineering, vol. 70, no. 3, pp. 719–730 (2021), DOI: 10.24425/aee.2021.137584.

[4] Nekoubin A., Soltani J., Dowlatshah M., *Multi-objective design optimization of five-phase fractional-slot concentrated-winding surface-mounted permanent-magnet machine*, Archives of Electrical Engineering, vol. 69, no. 4, pp. 873–889 (2020), DOI: 10.24425/aee.2020.134636.

[5] Geng S., Zhang Y., Qiu H., Yang C., Yi R., *Influence of harmonic voltage coupling on torque ripple of permanent magnet synchronous motor*, Archives of Electrical Engineering, vol. 68, no. 2, pp. 399–410 (2019), DOI: 10.24425/aee.2019.128276.

[6] Qiu H., Yu W., Li Y., Yang C., *Research on the influence of driving harmonic on electromagnetic field and temperature field of permanent magnet synchronous motor*, Archives of Electrical Engineering, vol. 66, no. 2, pp. 295–312 (2017), DOI: 10.1515/aee-2017-0022.

[7] Nekoubin A., Soltani J., Dowlatshahi M., *Comparative Analysis of Three-phase and Five-phase Permanent-magnet Motor Based on Finite Element Method*, Journal of Electrical Engineering and Technology, vol. 15, pp. 1705–1712 (2020), DOI: 10.1007/s42835-020-00444-3.

[8] Mekri F., Elghali S.B., Charpentier J.F., *Analysis, simulation and experimental strategies of 5-phase permanent magnet motor control*, Archives of Electrical Engineering, vol. 68, no. 3, pp. 629–641 (2019), DOI: 10.24425/aee.2019.129346.

[9] Iftikhar M.H., Park B.G., Kim J.W., *Design and analysis of a five-phase permanent-magnet synchronous motor for fault-tolerant drive*, Energies, vol. 14, no. 2, 514 (2021), DOI: 10.3390/en14020514.

[10] Chauhan S., Singh S.B., *Effects of Voltage Unbalance and Harmonics on 3-Phase Induction Motor During the Condition of Undervoltage and Overvoltage*, 6th International Conference on Signal Processing and Integrated Networks (SPIN), IEEE, pp. 1141–1146 (2019), DOI: 10.1109/SPIN.2019.8711753.

[11] Neves A.B.F., de Mendonça M.V.B., de Leles Ferreira Filho A., Rosa G.Z., *Effects of voltage unbalance and harmonic distortion on the torque and efficiency of a Three-Phase Induction Motor*, 17th International Conference on Harmonics and Quality of Power (ICHQP), pp. 943–948 (2016), DOI: 10.1109/ICHQP.2016.7783350.

[12] Quispe E.C., Lopez I.D., *Effects of unbalanced voltages on the energy performance of three phase induction motors*, IEEE Conf. on Power Electronics and Power Quality Applications, pp. 1–6 (2015), DOI: 10.1109/PEPQA.2015.7168237.

[13] Peng X., Liu Z., Jiang D., *A review of multiphase energy conversion in wind power generation*, Renewable and Sustainable Energy Reviews, vol. 147 (2021), DOI: 10.1016/j.rser.2021.111172.

[14] Tabasian R., Ghanbari M., Esmaeli A., Jannati M., *Control of three-phase induction machine drives during open-circuit fault: A review*, IETE Journal of Research, pp. 1–18 (2020), DOI: 10.1080/03772063.2020.1724833.

[15] Kebir A.A., Ayad M., Nacera Y., Kamel S., *Fault detection in fivephase permanent magnet synchronous machine affected by inter-turn short circuits*, 1st International Conference on Sustainable Renewable Energy Systems and Applications (ICSRESA) IEEE, pp. 1–6 (2019), DOI: 10.1109/ICSRESA49121.2019.9182312.

[16] Yan S., Tan S.C., Lee C.K., Chaudhuri B., Hui S.R., *Electric Springs for Reducing Power Imbalance in Three-Phase Power Systems*, IEEE Transactions on Power Electronics, vol. 30, pp. 3601–3609 (2015), DOI: 10.1109/TPEL.2014.2350001.